Journal of Organometallic Chemistry 694 (2009) 1223–1234

Contents lists available at ScienceDirect

Journal of Organometallic Chemistry

journal homepage: www.elsevier.com/locate/jorganchem

Diphospholyl and triphospholyl zirconium π-complexes: Ziegler–Natta oligomerization catalysts and reactive intermediates in P–C cage formation by hydrolysis

Jürgen Panhans, Frank W. Heinemann, Ulrich Zenneck *

Department Chemie and Pharmazie, Erlangen Catalysis Resource Center (ECRC), and Interdisciplinary Center for Molecular Materials (ICMM), Universität Erlangen-Nürnberg, Egerlandstr. 1, 91058 Erlangen, Germany

ARTICLE INFO

Article history:
Received 10 September 2008
Received in revised form 8 December 2008
Accepted 9 December 2008
Available online 25 December 2008

Dedicated to Professor Christoph Elschenbroich on the occasion of his 70th birthday.

Keywords:
Phosphorus
Zirconium
π-Complex
Ziegler–Natta catalyst
P–C cage compounds

ABSTRACT

2,4,5-Tri(*t*-butyl)-1,3-diphospholyl sodium salt (**2a**) and 3,5-di(*t*-butyl)-1,2,4-triphospholyl sodium salt (**3a**) react with $ZrCl_4$ and $CpZrCl_3$ to form (η^5-2,4,5-tri(*t*-butyl)-1,3-diphospholyl)$ZrCl_3$ (**4**), Cp(η^5-2,4,5-tri(*t*-butyl)-1,3-diphospholyl)$ZrCl_2$ (**5**), and Cp(η^5-3,5-di(*t*-butyl)-1,2,4-triphospholyl)$ZrCl_2$ (**6**) in the complete absence of water, respectively. Surprisingly, bent sandwich complex **6** exhibits the NMR spectroscopic characteristics of a hindered ring ligand rotation but the cyclopentadienyl ligand of **5** rotates freely in the NMR time scale in spite of the superior space demand of its 2,4,5-tri(*t*-butyl)-1,3-diphospholyl ligand. This contradiction is discussed on the basis of an attractive interligand P–C interaction between homo- and heterocyclic π-ligands, which is stronger for **6**. Water even in trace amounts present in the reaction mixture changes the course of the reactions completely. No zirconium π-complexes are accessible this way, but only oligo- or polycyclic organophosphorus compounds. Compound **3a** and $ZrCl_4$ form the asymmetric tricyclic $P_6(t\text{-BuC})_4H_2$ isomer **8** with two P=C double bonds as a dimer of 1,2,4-triphosphol. It is accompanied by small amounts of HCl addition product **9**, where one of the P=C double bonds is eliminated. Compound **8** contains six, and **9** eight stereogenic centers, but both form one pair of enantiomers each only. A single stereoisomer of $P_6(t\text{-BuC})_4H_2$ cage **10** is formed if (1-trimethylstannyl)-3,5-di(*t*-butyl)-1,2,4-triphosphol **3b** is used as the $P_3(t\text{-BuC})_2$ source in combination with Cp^*ZrCl_3 in the presence of trace amounts of water. Compound **10** is a *meso-compound,* which is composed by dimerization of either two homochiral units of (*R*)-3,5-di(*t*-butyl)-1,2,4-triphosphol **3c***R* or by two units of its *S*-enantiomer **3c***S*. No trace of cyclic addition products has been identified, which would represent the heterochiral combination of enantiomers **3c***R* + **3c***S*. P_2- and P_3-zirconocene dichloride derivatives **5** and **6** have been tested as Ziegler–Natta alkene oligomerization catalysts. Both are catalytically active with 1-hexene as the substrate, but cannot compete with the activity of the phosphorus-free original catalyst Cp_2ZrCl_2.

1. Introduction

Cp_2ZrCl_2 and its derivatives are excellent Ziegler–Natta catalysts with a high potential in practical applications [1]. One approach of modifying the properties of this type of compounds significantly is the introduction of phosphorus atoms into the ring ligands, which results in the transformation of one or both cyclopentadienyls into phospholyl derivatives [2]. The main catalytic application of (π-phospholyl)Zr complexes is polymerization or oligomerization of olefins with or without the help of methylalumoxane (MAO) as a co-catalyst [3], including 1-hexene [4]. Catalytic ring opening of epoxides with TMSCl is another application of (π-phospholyl)Zr complexes [5]. In significant contrast to that, only one patent appeared in the literature dealing with a (π-1,3-diphospholyl)$_2ZrCl_2$ species as a catalyst for olefin polymerization [6], however, no complete preparative results have been published to date about diphospholyl zirconium complexes or other zirconocene derivatives with more than two phosphorus atoms being part of the five-membered ring ligands. With this paper we report about 1,3-diphospholyl and 1,2,4-triphospholyl zirconium π-complexes and our attempts for using them as Ziegler–Natta catalysts to fill that gap.

On the other hand, the marked oxophilicity of Zr(IV) π-complexes leads to a strong tendency of those compounds to react even with traces of water or air to form oxo, hydroxo, or aquo species of the metal and follow-up products of the ligands. In the case of the di- and triphospholyl zirconium complexes we report in this paper, this requires very careful preparative, workup and handling procedures, but it opens at the same time a new gate to polycyclic P–C

* Corresponding author. Tel.: +49 9131 852 7464; fax: +49 9131 852 7367.
E-mail address: ulrich.zenneck@chemie.uni-erlangen.de (U. Zenneck).

0022-328X/$ - see front matter © 2008 Elsevier B.V. All rights reserved.
doi:10.1016/j.jorganchem.2008.12.026

cage compounds by cyclic addition reactions of the released and partially modified ligands. We are deeply interested in P–C cage chemistry on the basis of unsaturated P-heterocycles, as we detected an inherent and very high diastereoselectivity for chiral species [7], which led us actually to the novel class of optically active cage-chiral P–C cage compounds [8].

2. Results and discussion

2.1. Preparation of π-complexes

Becker et al. have shown that the reduction of stable phosphaalkene $Me_3SiP{=}C(OSiMe_3)(t\text{-Bu})$ (**1**) with elemental alkali metals M or suitable metal organic compounds MR_n leads to the formation of salt mixtures M[2,4,5-tri(*t*-butyl)-1,3-diphospholyl] (**2**) and M[3,5-di(*t*-butyl)-1,2,4-triphospholyl] (**3**) as the main product [9]. Such mixtures are separable through repeated fractional crystallization of the sodium salts **2a**/**3a** from THF [10] (Scheme 1).

The separated sodium salts **2a** and **3a** have been reacted with $ZrCl_4$ and $CpZrCl_3$. Target products (η^5-2,4,5-tri(*t*-butyl)-1,3-diphospholyl)$ZrCl_3$ (**4**), Cp(η^5-2,4,5-tri(*t*-butyl)-1,3-diphospholyl)$ZrCl_2$ (**5**), and Cp(η^5-3,5-di(*t*-butyl)-1,2,4-triphospholyl)$ZrCl_2$ (**6**) were isolated and characterized from the respective reaction mixtures in the complete absence of water only (Scheme 2). Other products formed from the same starting materials or closely related ones like (η^5-3,5-di(*t*-butyl)-1,2,4-triphospholyl)$ZrCl_3$, Cp^*(η^5-3,5-di(*t*-butyl)-1,2,4-triphospholyl)$ZrCl_2$, or the Hf-analogue of (**4**) (η^5-2,4,5-tri(*t*-butyl)-1,3-diphospholyl)$HfCl_3$ have been observed only spectroscopically, but were too reactive or unstable in our hands for complete characterization. Moisture even in trace amounts present in the reaction mixtures or prolonged reaction times change the course of the reactions completely. Some oligo- and polycyclic organophosphorus compounds are accessible in preparative useful amounts in that cases, based on the hydrolysis products of the π-ligands (*vide infra*).

As a consequence, the handling of **4**, **5,** and **6** requires careful exclusion of air and moisture. 1,3-Diphospholyl complexes **4** and **5**, allow recrystallization from refluxing *n*-hexane, but 1,2,4-triphospholyl species **6** decomposes when solutions are heated up beyond room temperature and (1,2,4-triphospholyl)$ZrCl_3$ has been observed only as a reaction intermediate (*vide infra*). We relate the relative stabilization of the 1,3-diphospholyl complexes mainly to a shielding effect of the three *t*-Bu substituents of the heterocycle. $^{31}P\{^1H\}$ NMR spectroscopy of π-complexes **4–6** result in single line spectra for diphospholyl complexes **4** and **5** and AB_2 spin systems for **6** and those 1,2,4-triphospolyl complexes, which are only observable spectroscopically (Table 1, Supporting information).

The chemical shifts of the ^{31}P NMR signals and the $^2J_{AB}$ values for the 1,2,4-triphospholyl complexes are close to the observations for π-complexes of other electron-poor transition metal ions like Ti^{2+} [11], Sc^{3+}, or Y^{3+} [12]. Replacement of one of the chlorides of **4** or (1,2,4-triphospholyl)$ZrCl_3$ by the Cp ligands of **5** and **6** or a Cp^* cause a high-field shift of the ^{31}P NMR absorptions of the respective heterocycles. The effect is significantly stronger for the B nuclei than for the single A nucleus of the triphospholyl ligands.

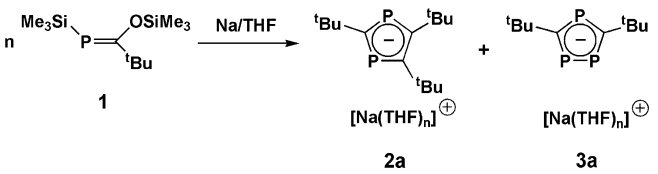

Scheme 1. Preparation of sodium salt mixture **2a** + **3a.**

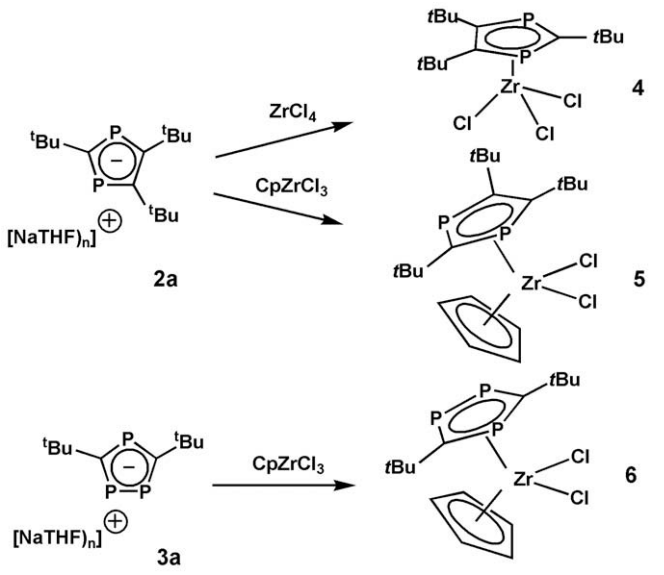

Scheme 2. Preparation of (η^5-1,3-diphosphophospholyl)Zr complexes **4** and **5** and (η^5-1,2,4-triphosphophospholyl)Zr complex **6**.

Table 1
$^{31}P\{^1H\}$ NMR data (121.49 MHz, toluene-d^8, RT) of 1,3-diphospholyl and 1,2,4-triphospholyl zirconium π-complexes.

Compound	δ_A (multipl.)	δ_B (multipl.)	$^2J_{AB}$ (Hz)
(η^5-(*t*-BuC)$_3$-1,3-P_2)$ZrCl_3$ (**4**)	260.3 (s)	–	
Cp(η^5-(*t*-BuC)$_3$-1,3-P_2)$ZrCl_2$ (**5**)	236.7 (s)	–	
(η^5-(*t*-BuC)$_2$-1,2,4-P_3)$ZrCl_3$	310.8 (t)	323.3 (d)	55.5
Cp(η^5-(*t*-BuC)$_2$-1,2,4-P_3)$ZrCl_2$ (**6**)	282.5 (t)	260.2 (d)	51.2
Cp^*(η^5-(*t*-BuC)$_2$-1,2,4-P_3)$ZrCl_2$	285.0 (t)	252.5 (d)	55

As a consequence the relative positions of A and B nuclei is reversed for the Cp and Cp^* species with respect to (η^5-1,2,4-triphospholyl)$ZrCl_3$. A strong influence of the exact position of the other π-ligand on the δ (^{31}P) values of sandwich complex (η^5-3,5-di(*t*-butyl)-1,2,4-triphospholyl)$_2$Ru has been elucidated from detailed DNMR investigations [13]. With respect to the bent sandwich complexes of this paper, the finding indicates a close contact of the P_B-nuclei with the Cp or Cp^* ligands, but a weaker interaction between P_A and the homocyclic π-ligands. No peculiarities have been observed in the ^1H and $^{13}C\{^1H\}$ NMR spectra of **5** in solution. The cyclopentadienyl hydrogen and carbon atoms form sharp singlets. This is in accord with related NMR spectroscopic observations on Cp(η^5-3,5-di(*t*-butyl)-1,2,4-triphospholyl)Fe [14] or Cp(η^4-1-phenyl-3,5-di(*t*-butyl)-1,2,4-triphosphol)Co, [15] for example, where a rapid ring ligand rotation explains the NMR results.

To our surprise, the NMR spectra of Cp(1,2,4-triphospholyl)$ZrCl_2$ (**6**) do not fit to this scheme. Both, ^1H and $^{13}C\{^1H\}$ NMR signals of the Cp ligand split into two sets of signals in the ratio 2:3, (Fig. 1; Supplementary material for ^{13}C) thus two of the five C–H moieties of the Cp ring have been significantly discriminated by the heterocyclic co-ligand and just that ^{13}C signal is split into a triplet with a P–C coupling constant of 2.2 Hz. To analyze the problem, models for the conformational ground states **5A** and **6A** were developed on the basis of their molecular structures in the solid state (Fig. 2). From the X-ray data one can identify two CH units of the Cp to be in close contact with one P-lone pair of the 1,3-diphospholyl ligand for **5A**, and two CH-moieties of **6A** have a related close contact with the two lone pairs of the 1,2-P_2-moiety. The nearest interligand P–C distances range from 325 to 335 Å. This is 15–25 Å smaller than the sum of the van der Waals radii

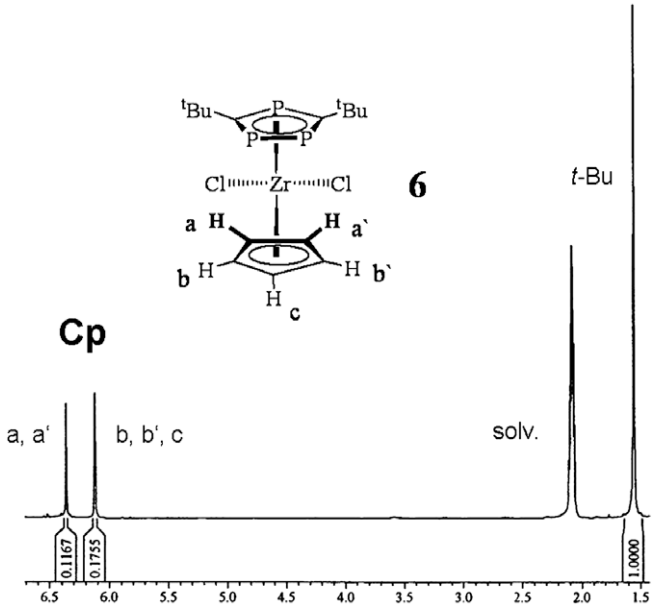

Fig. 1. ^{1}H NMR spectrum of Cp(η^5-3,5-di(*t*-butyl)-1,2,4-triphospholyl)$ZrCl_2$ (**6**). (300 MHz, solv. = toluene-d^8, RT).

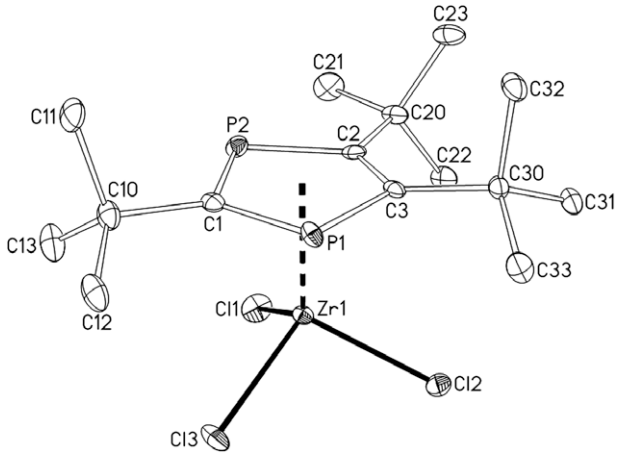

Fig. 3. Molecular structure of (η^5-2,4,5-tri(*t*-butyl)-1,3-diphospholyl)$ZrCl_3$ (**4**), in the solid state; hydrogen atoms are omitted for clarity. Selected bond distances [pm] and angles [°]: Zr(1)–Cl(1): 236.09(9); Zr(1)–Cl(2): 236.36(8); Zr(1)–Cl(3): 235.24(9); Zr(1)–C(1): 264.2(3); Zr(1) –C(2): 261.7(3); Zr(1) –C(3): 265.7(3); Zr(1)–P(1): 276.09(9); Zr(1)–P(2): 277.49(9); Ct(0)–Zr–Cl(1): 117.20; Ct(0)–Zr–Cl(2): 115.90; Ct(0)–Zr–Cl(3): 118.79; Cl(3)–Zr(1)–Cl(1): 98.93(3); Cl(3)–Zr(1)–Cl(2): 99.47(3); Cl(1)–Zr(1)–Cl(2): 103.54(3). Ct(0) = centroid of 1,3-diphospholyl ring.

of phosphorus and carbon atoms (350 pm) [16], but no unusual short interligand P–H distances have been identified (*vide infra*).

To relate the models with the experimental NMR spectra, free rotation of the Cp ligand of **5** has to be assumed in combination with a rapid pendulum movement of the 1,3-diphospholyl ligand to equilibrate the two chemically inequivalent phosphorus atoms of **5A** in the NMR timescale. A complete rotation of the heterocycle is not required to explain the spectra and seems to be unlikely, as two adjacent *t*-butyl groups would have to pass together the narrow zone of the bent sandwich complex as a competitive process to the pendulum movement where only one *t*-butyl group passes the Cp co-ligand at a time. The static model **6A** fits completely to the observed NMR spectra of **6** in solution. It explains the 2:3 intensity of the ^{1}H and ^{13}C{^{1}H} Cp ligand signals, the P–C interligand coupling, and the stronger influence of the Cp ligand on the chemical shift of the two P_B nuclei. On the other hand, a free rotating 1,2,4-triphospholyl ligand of **6** in combination with a static Cp would create the same NMR spin systems, but this constellation seems to be very unlikely as the P-heterocycle carries the bulky substituents and should be substantially more hindered in its

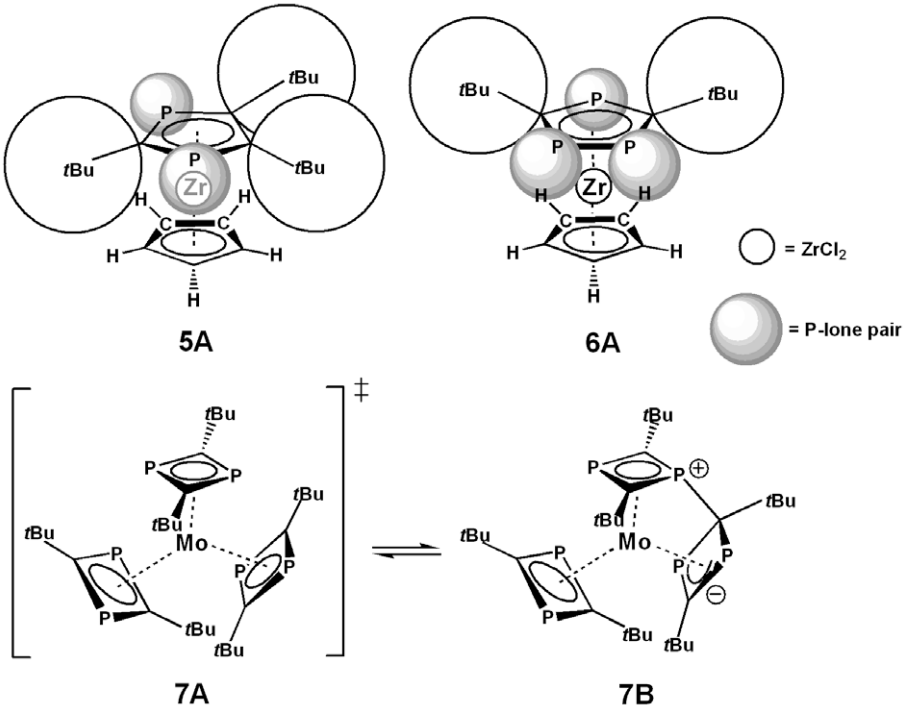

Fig. 2. Models of the conformational ground states **5A** and **6A** based on the molecular structures of **5** and **6** in the solid state (top) and interligand P–C bond formation of tris(2,4-di-*t*-butyl-1,3-diphosphete)Mo **7** (bottom).

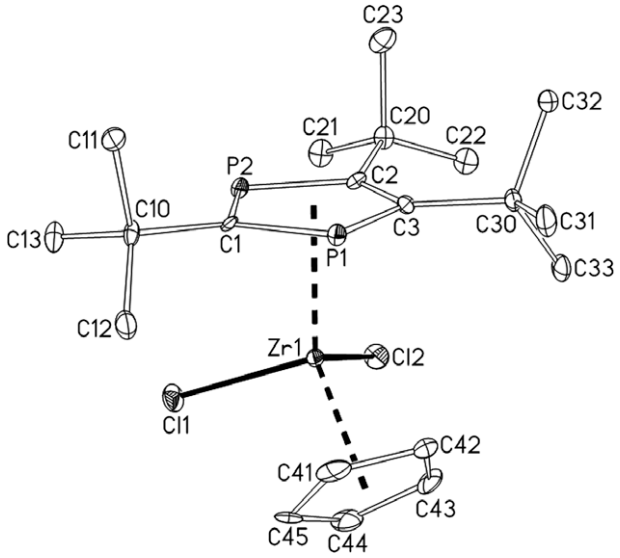

Fig. 4. Molecular structure of Cp(η^5-2,4,5-tri(*t*-butyl)-1,3-diphospholyl)$ZrCl_2$ (**5**), in the solid state; hydrogen atoms are omitted for clarity. Selected bond distances [pm] and angles [°]: Zr(1)–Cl(1): 244.41(1); Zr(1)–Cl(2): 243.95(1); Zr(1)–Ct(1): 237.3; Zr(1)–Ct(2): 222.5; Ct(1)–Zr(1)–Cl(1): 110.22; Ct(1)–Zr(1)–Cl(2): 107.27; Ct(1)–Zr(1)–Ct(2): 132.63; Ct(2)–Zr(1)–Cl(1): 102.32; Ct(2)–Zr(1)–Cl(2): 103.92; Cl(1)–Zr(1)–Cl(2): 93.62. Ct(1) = centroid 1,3-diphospholyl; Ct(2) = centroid Cp ligand.

mobility than the Cp ring. A third alternative view would be a Cp ring slippage towards η^3-co-ordination, but **6** lacks the excess of electron density at the central metal which is required for that process [17]. Neither the δ (^{13}C) value of the separated $(CH)_2$-unit, nor its P–C coupling constant are compatible with η^3-co-ordination.

The statement of a free rotating Cp ligand of **5** and an obviously hindered Cp ligand rotation of **6** is not easily understood, as the repulsive interaction between the C-H units of the cyclopentadienyls and the *t*-butyl substituents of the heterocycles are not regarded as very high and should be even smaller for **6** (Fig. 2). Additionally, a hindered C_5H_5 ligand rotation in solution at room temperature would be a novelty. All reports we found in the literature for a hindered Cp ligand rotation of bent sandwich Cp_2ZrX_2

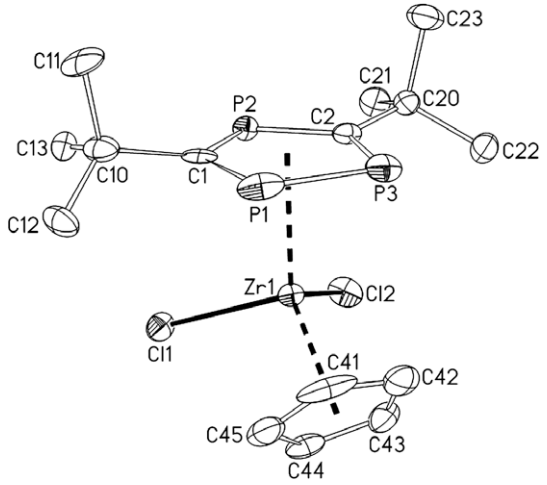

Fig. 5. Molecular structure of Cp(η^5-3,5-di(*t*-butyl)-1,2,4-triphospholyl)$ZrCl_2$ (**6**), in the solid state; hydrogen atoms are omitted for clarity. Selected bond distances [pm] and angles [°]: Zr–Cl(1): 243.50(2); Zr–Cl(2): 243.03(3); Zr–Ct(1): 240.6; Zr–Ct(2): 220.6; Ct(1)–Zr–Cl(1): Ct(1)–Zr–Cl(1): 107.24; Ct(1)–Zr–Cl(2): 106.84; Ct(1)–Zr–Ct(2): 133.2; Ct(2)–Zr–Cl(1): 104.13; Ct(2)–Zr–Cl(2): 104.68; Cl(1)–Zr–Cl(2): 93.93(7). Ct(1) = centroid 1,2,4-triphospholyl; Ct(2) = centroid Cp ligand.

complexes concern such species, where both ring ligands carry bulky substituents [18].

Fluxional behavior of *t*-butyl group substituted 1,3-diphospholyl and 1,2,4-triphospholyl ligands in sandwich complexes has been analyzed by ^{31}P NMR spectroscopy for some tetra- and hexaphosphametallocenes with Fe, Ru, Sn, and Pb [13,19,20] central metal atoms. It is explained mainly by *t*-butyl substituent repulsion between the ligands. The observations include interring P–P coupling of P_6-ferrocene and P_6-ruthenocene. Due to a lack of experimental data, no direct relation of the activation parameters for ring rotation between 1,3-diphospholyl and 1,2,4-triphospholyl ligands can be defined, but dynamic NMR studies on symmetry and size related 1,3-bis- and 1,2,4-tris-trimethylsilyl-cyclopentadienyl complexes of the general types Cp_2M and Cp_2MCl_2 give clear evidence for the dominating influence of the three bulky substituents of the 1,2,4-tris-trimethylsilyl ligand in both cases [21]. Examples for tetrahedral oligophosphametallocenes like **5** and **6** with two strongly tilted η^5-ring ligands and two sigma ligands are not available to date. (η^5-3,5-Di(*t*-butyl)-1,2,4-triphospholyl)$_3$Sc comes close to the topology of **6**, it is fluxional, exhibits interring P–P-coupling, but no complete analysis of the NMR spectra was possible [12]. Topologically even closer related is Cp^*(η^3-2,4,5-tri(*t*-butyl)-1,3-diphospholyl)$Mo(CO)_2$ [22], however, the heterocycle is η^3-bound and its Cp^* ligand rotates free in the NMR time scale. An interligand P_{ring}–C_{ring} coupling for a π-complex has been reported in one example only. It concerns (η^5-2,4,5-tri(*t*-butyl)-1,3-diphospholyl)(η^5-cyclooctadienyl)Ru, where the $^{13}C\{^1H\}$ signals of two if the five dienyl carbon atoms are split by 4.7 Hz into a triplet again by the two P-atoms of the heterocycle [23].

A summary of the information available in the literature leads to the conclusion that both, hindered or free rotation of π-bound 1,3-diphospholyl and 1,2,4-triphospholyl ligands with *t*-butyl C-substituents has been identified by NMR spectroscopy for sandwich and half sandwich complex examples. Repulsive interaction between bulky ring ligand substituents in close proximity was always identified as the most important factor for the control of the molecular dynamics of such compounds, however, **6** does not fit to that interpretation! Unluckily, its limited thermal stability did not allow analyzing the contradictory results by dynamic NMR spectroscopy.

A comprehensive approach for the identification of the reasons for the hindered conformational flexibility of some π-complexes led to attractive electronic interactions between some molecular building blocks, which might dominate the dynamic effects in specific cases. This accounts for the rotation of the exocyclic double bond of fulvene derivatives in some cationic Cp(fulvene)Fe^+ and (C_4R_4)(fulvene)Co^+ complexes, for example, which is controlled by a strong interaction of the side chain α-carbon atom with the transition metal [24]. Tris(2,4-di-*t*-butyl-1,3-diphosphete)Mo **7** might serve as a model to elucidate an attractive force between the ring ligands of **6**, which has the potential to explain a hindered Cp ligand rotation in that specific case. Compound **7** was first described as the triangular π-complex **7A** with an unexplained short distance of 215.1 pm between one phosphorus atom and a ring carbon atom of one of the neighboring ligands [25]. A reinvestigation at low temperature, however, led to the identification of **7B** as the ground state of the molecule, where a P–C single bond between two ligands with a length of 198.8 pm is formed at that specific position [26]. Compound **7A** serves as the transition state in equilibrium between **7B** and its mirror image only (Fig. 2). The interligand P–C bond formation of **7B** was explained by the ambiphilicity of its P-heterocyclic ligands. A nucleophilic attack of a P-lone pair leads to a bond with an electrophilic ring carbon atom of the other ligand. A related constellation is realized two times in **6**, but only one of the P-lone pairs of **5** can interact this way with the Cp ring. The nucleophilicity of P-lone pairs should not differ much between

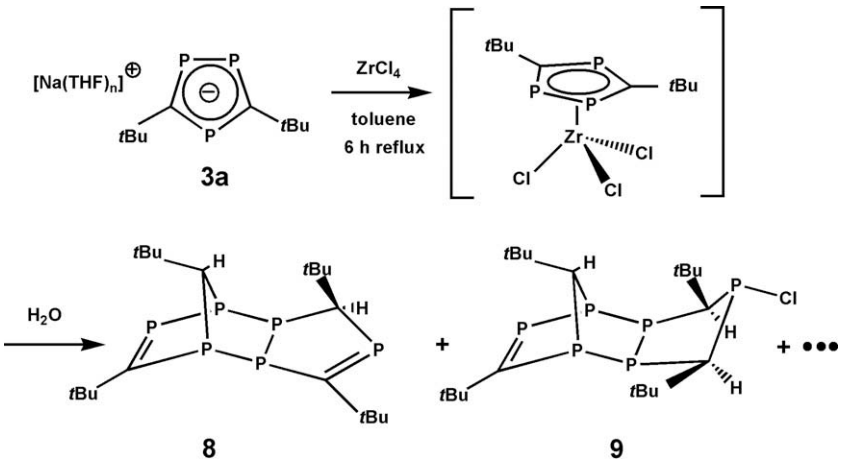

Scheme 3. Preparation of tricyclic organophosphorus compounds **8** and **9**.

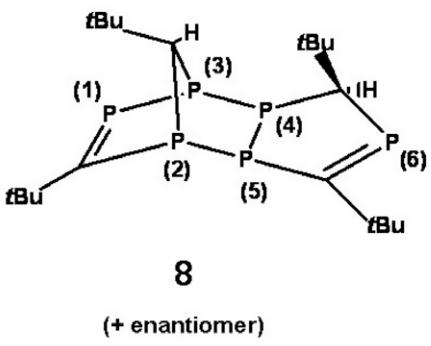

$^{1}J_{PP}$ or $^{2}J_{PP}$ [Hz]

δ [ppm]	P(1)	P(2)	P(3)	P(4)	P(5)	P(6)
317, P(1)			277			
27, P(2)					317	
30, P(3)	277			309		
-18, P(4)			309		381	31.5
18, P(5)		317		381		
330, P(6)				31.5		

Fig. 6. ^{31}P NMR shift and coupling matrix data of **8**.

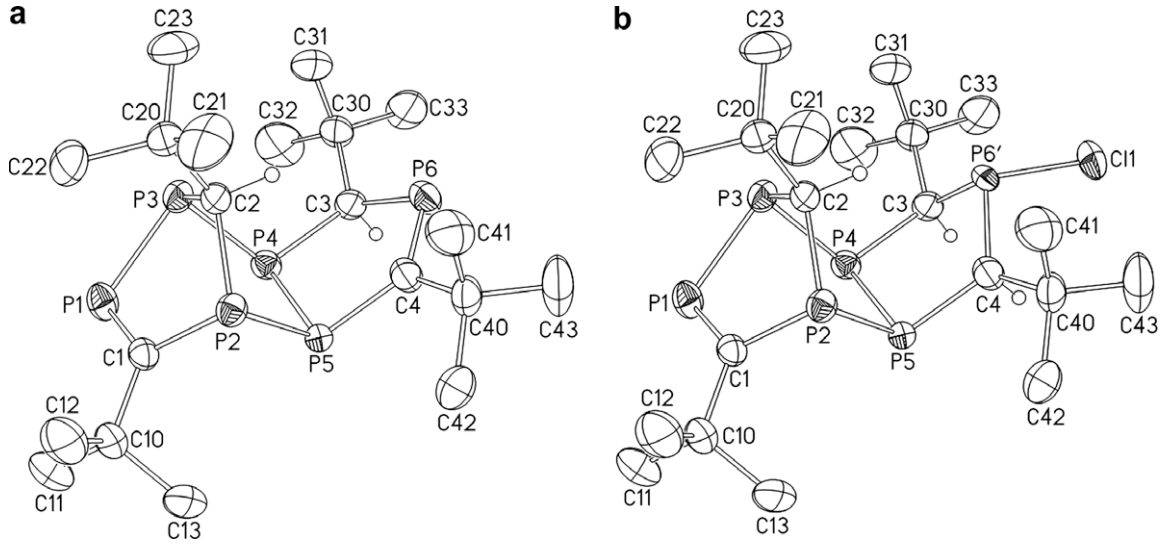

Fig. 7. Molecular structure of $C_{20}H_{38}P_6$ (**8**) (a) and $C_{20}H_{39}ClP_6$ (**9**) (b) in the solid state as determined from a mixed crystal of both components, containing 11% of **9**; *t*-Bu group hydrogen atoms are omitted for clarity. Selected bond distances [pm] and angles [°] for **8**: P(1)–C(1): 168.8(3); P(6)–C(4): 167.8(4); P(6)–C(3): 184.5(4); P(1)–P(3): 219.98(1); P(2)–P(5): 224.80(1); P(3)–P(4): 221.70(11); P(4)–P(5): 222.98(19); P(2)–C(1): 183.5(3); P(1)–P(3)–P(4): 88.71(4); C(1)–P(2)–P(5): 94.04(9); C(4)–P(6)–C(3): 104.08(17).

four- or five-membered P-heterocyclic π-ligands, but the electrophilicity of Cp ring carbon atoms is believed to be weaker as in the case of 1,3-diphosphetes due to the lack of phosphorus atoms as ring elements. In the light of this argument, an attractive force is likely to exist between the ligands of **5** and **6**, with a preference for **6** because of the double interaction. We are working out and checking this model actually by theoretical investigations on a high level, which include the complete *t*-butyl substituents.

X-ray structure investigations of **4**, **5**, and **6** supplied information of the molecular structures of the compounds in the solid state. Crystals suitable for X-ray diffraction studies have been obtained from *n*-hexane in all three cases. Compound **4** crystallizes in yellow prisms in the space group $P2_1/c$. Unlike its carba analogues $CpZrCl_3$ and Cp^*ZrCl_3, crystalline **4** consists of independent molecular complex units with the heterocycle as a η^5-bonded π-ligand and three chloride σ-ligands of the central zirconium atom (Fig. 3). $CpZrCl_3$ forms a Cl-bridged polymer [27] and Cp^*ZrCl_3 a Cl-bridged dimer [28]. There are no unusual short interatomic distances between the molecules of **4**, no peculiarities are connected with the bond distances and angles of the (η^5-1,3-diphospholyl)Zr moiety. The Zr–Cl distances of **4** are shortened by 5.5–6.7 pm with respect to the non-bridging Zr–Cl bonds of $CpZrCl_3$, but the Zr-centroid distance of **4** is expanded by 7.2 pm. The latter is due to the superior covalent radius of the P-atoms of the heterocycle over that of the carbon atoms. The three *t*-Bu groups may contribute to the effect by their big volume.

Crystallization from *n*-hexane leads to irregular shaped yellow crystals of Cp(2,4,5-tri(*t*-butyl)-1,3-diphospholyl)$ZrCl_2$ (**5**) which were suitable for X-ray diffraction. The compound crystallizes in the orthorhombic space group $P2_12_12_1$. As for **4** it consists of neutral molecules with no close intermolecular contacts (Fig. 4). The ring ligands are planar and their relative orientation forms an almost staggered bent sandwich complex unit with P1 in closest proximity to the Cp ligand. The Zr–Cl bonding distances are slightly enhanced in relation to **4**, but almost identical with those of its carba analogue Cp_2ZrCl_2 (244.6 pm und 243.6) [29]. The distance between the zirconium atom and the centroid of the 1,3-diphospholyl ring exceeds that of the Cp ring by 8%. This is a substantial increase. We relate it to the three *t*-Bu substituents of the heterocycle. The bond angle between the chloro ligands serves as a second monitor for the enhanced steric pressure within **5**. The angle Cl(1)–Zr(1)–Cl(2) = 93.6° is compressed by 5–10° if compared to the Cl–Zr–Cl angles of **4**. In spite of the repulsive interaction of the *t*-butyl 1,3-diphospholyl substituents with the other molecular building blocks of **5**, two unusual short distances have been found between its cyclic ligands. The non-bonding P–C distances P1–C41 = 330.2 (4) pm and P1–C42 = 333.7 (4) pm fall substantially short with respect to the sum of the van der Waals radii (350 pm) [16]. As discussed with the NMR data, we regard this selective shortening of P–C distances as a consequence of an attractive P–C interligand interaction.

Crystals of Cp(3,5-di(*t*-butyl)-1,2,4-triphospholyl)$ZrCl_2$ (**6**) were grown from a saturated *n*-hexane solution at room temperature. The compound forms yellow needles in the orthorhombic space group $P2_12_12_1$, it is characterized by neutral molecules with no close intermolecular contacts (Fig. 5). As observed for **5**, the molecular structure of **6** in the crystal exhibits unusual short interligand P–C distances. The data concern P1–C41 = 324.5 (9) pm and P3–C42 = 335.0 (9) pm. The shortening effect of 25.5 and 15.0 pm with respect to the sum of the van der Waals radii grants a close electronic contact between the lone pairs of P1 and P3 and the p_z-orbitals of C41 and C42, respectively, across space between the ring ligands. It serves as a model for the understanding of the observed ^{31}P–^{13}C NMR coupling along this route and for the hindered Cp ligand rotation in solution.

2.2. Preparation of oligo- and polycyclic organophosphorus compounds through zirconium π-complex intermediates

All reactions of the zirconium complexes $ZrCl_4$, $CpZrCl_3$, and Cp^*ZrCl_3 performed with the separated sodium salts **2a** and **3a** or 1-trimethylstannyl-3,5-di(*t*-butyl)-1,2,4-triphosphole **3b** [15] yielded oligo- or polycyclic organophosphorus compounds which can be related in most cases to cyclic addition products of the related protonated P-heterocycles. Mixtures of organophosphorus products are formed normally as indicated by ^{31}P NMR spectroscopy from the reaction mixtures which proved to be difficult to work up and characterize. As outlined above, the reported zirconium π-complexes can only exist in the absence of moisture and air. ^{31}P NMR monitoring of several reaction mixtures gave hints on processes, which consume the π-complexes after some time at elevated temperature even in the absence of these factors and more reactive complexes did not allow their isolation but only the observation of reactive intermediates. So we turned the experiments systematically in the direction of preparing novel organophosphorus compounds this way. Direct hydrolysis of the isolated 1,3-diphospholyl and 1,2,4-triphospholyl zirconium π-complexes **4–6** by addition of water, water deactivated alumina, or silica to solutions of the compounds led directly to the compounds of interest, but no preparative useful reactions were identified this way.

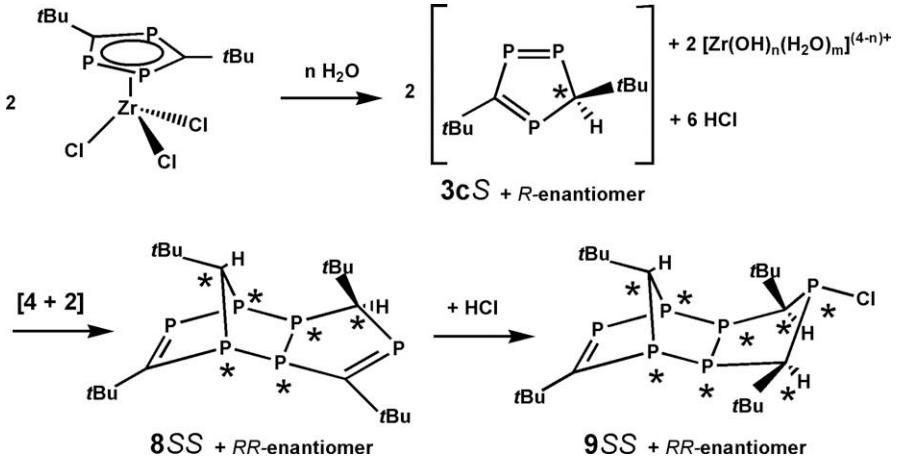

Scheme 4. Mechanistic considerations about the formation of single pairs of enantiomers of compounds **8** and **9**.

Equimolar amounts of **3a** and $ZrCl_4$ in refluxing toluene form the twofold unsaturated tricyclic $P_6(t\text{-BuC})_4H_2$ isomer **8** as the main product, its HCl addition product **9,** and a completely saturated $P_6(t\text{-BuC})_4H_2$ isomer in smaller amounts which has been obtained earlier by a different synthetic route [30] (Scheme 3). The proposed π-complex intermediate (η^5-3,5-di(*t*-butyl)-1,2,4-triphospholyl)$ZrCl_3$ was not observed in the reaction mixture at toluene reflux conditions, but at room temperature only and reaction times of less than an hour. A complete set of spectroscopic parameters of (η^5-3,5-di(*t*-butyl)-1,2,4-triphospholyl)$ZrCl_3$ has been determined from those experiments (Table 1). Chromatographic workup of the mixture of organophosphorus compounds on water deactivated silica (5% water) with *n*-hexane completed hydrolysis and allowed the separation of **8** and **9** on the one side and the saturated $P_6(t\text{-BuC})_4H_2$ isomer from further organophosphorus compounds which have not been identified yet. Repeated chromatography allowed preparation of even highly enriched samples of either **8** or **9** in solution, but yielded no analytically pure compounds. Recrystallization did not separate **8** and **9** completely due to the formation of mixed crystals. The isolated yields of the mixtures **8 + 9** were always around 30% but their relative concentration changed from run to run. The main component **8** is an asymmetric compound with six stereogenic centers, but it generates only a single set of six $^{31}P\{^1H\}$ NMR signals, all with the same integral intensity (Fig. 6). Six signals are found for side product **9** as well, but it exhibits only one P═C unit.

The data of **8** suggest the formation of a single pair of enantiomers of an organophosphorus compound with six inequivalent phosphorus atoms. Two of them form P═C double bonds, the others exhibit only single P–C and P–P bonds for the phosphorus atoms. This can be understood on the basis of a cyclic addition reaction of two enantiomeric 3,5-di(*t*-Bu)-1,2,4-triphosphole molecules **3c** (*vide infra*). The reaction must have taken place in a way which prevented the formation of NMR spectroscopic distinguishable diastereomers. Related observations have been made with some other cyclic addition processes in this field of chemistry by our group [7]. ^1H NMR and FD MS led to the same interpretation.

Crystals suitable for X-ray diffraction studies in space group $P2_1/n$ have been obtained from *n*-hexane solution at −18 °C. The crystalline material investigated consisted of a mixed crystal of molecular **8** with its HCl addition product **9** in the ratio 0.89:0.11, both occupying the same crystallographic positions statistically (Fig. 7).

The molecular structure of **8** in the solid state consists of tricyclic chiral 1,2,4,5,6,8-hexaphospha-3,7,9,10-tetra(*tert*-butyl)-tricyclo-[4.3.3.0]-3,9-decadiene as a pair of enantiomers. As suggested by the NMR parameters, it contains six chemically distinguishable P-atoms including two P═C double bonds: P(1)═C(1) and P(6)═C(4) which were identified by their characteristic bond distances of 168.8 and 167.8 pm and their planar carbon atoms. All observed P–P and P–C single bond distances are in the typical range for such compounds again [7]. Stereochemistry of **9** is identical with that of **8** for the tricyclic structure, but two additional stereogenic centers for C(4) and P(6) have been generated by hydrogen (C(4)) and chlorine (P(6)) atom addition in a completely diastereoselective manner. More of the structural details of **9** shall not be discussed because of its small contribution to the X-ray diffraction data of the crystal.

The tricyclic structure of **8** and **9** resembles that of the *exo-dimer* of 2,4,5-tri(*t*-butyl)-1,3-diphosphole [31], which was prepared in the absence of transition metals, but the principal mechanistic considerations are the same. Both form [4+2] cyclic addition *exo*-dimers. Due to their closely related stereochemistry, **9** is believed to be a direct HCl addition product of **8** (Scheme 4).

The pairs of enantiomers identified for **8** and **9** prove a high diastereoselectivity of the cyclic addition process of the two 1,2,4-triphosphole molecules **3c**. Only homochiral triphospholes dimerize, to form **8***SS* and **8***RR*, respectively, as a pair of enantiomers and the related enantiomers of **9** in the successive step. No cyclic addition product between heterochiral **3c***S* and **3c***R* were identified among the products.

Two questions are open at the moment and we are working on understanding them in the future.

– We have not yet identified unambiguously the source of the hydrogen atoms for the formation of 1,2,4-triphosphole **3c**. Part of it is obviously supplied by the water content of the glassware used and the chemicals, but the yield of **8** + **9** is too high to rely on that resource only. A hint in that direction is given by changing ratios of **8** vs. **9** in different runs of the experiments. The

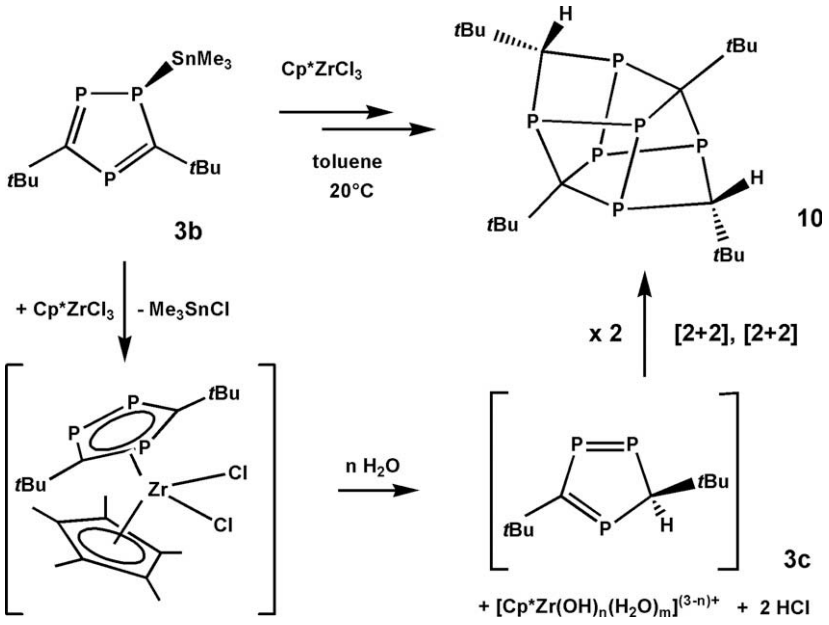

Scheme 5. Preparation and proposed mechanism of the formation of saturated $P_6(t\text{-BuC})_4H_2$ cage isomer **10**.

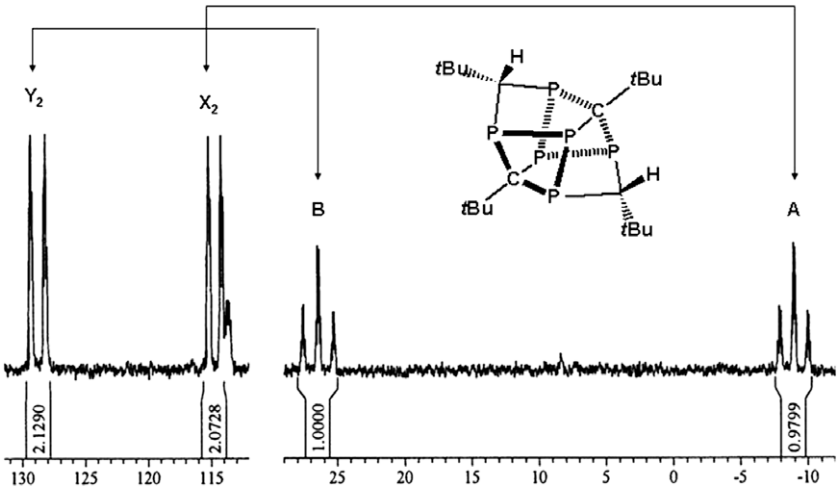

Fig. 8. $^{31}P\{^{1}H\}$ NMR spectrum of $C_{20}H_{38}P_6$ **10** (121.5 MHz, toluene-d^8, RT, z = impurity). NMR parameters: $\delta_A = -8.9$, $\delta_X = 114.7$ ppm, $^{1}J_{AX} = 124$ Hz; $\delta_B = 26.4$, $\delta_Y = 128.7$ ppm, $^{1}J_{BY} = 140$ Hz.

availability of HCl and thus the effectivity of the transformation of **8** into **9** is most probably due to the amount of water being present in the specific run. We have the impression 1,2,4-triphospholyl radicals play an additional role as a hydrogen abstracting reagent from the C–H acidic solvent toluene to form **3c** in the reaction besides anion protonation.

– Free 1,2,4-triphosphole **3c** was most probably present in the experiments of Nixon et al. when they prepared a saturated $P_6(t\text{-BuC})_4H_2$ cage isomer of **8**, which is always present in our experiments as a side product in small amounts in the starting material **3a**. This cage was related to the *endo*-cyclic addition product of two molecules of **3c** [30]. We take this as a hint on the important role of the zirconium component in the experiments reported here. The transition metal obviously determines the orientation of the cyclic addition step, but we do not know how in the moment. Proof for the intermediacy of a triphospholyl zirconium π-complex in the formation of tricyclic **8** was given by the direct synthetic route. Direct hydrolysis of a *n*-hexane solution of Cp(η^5-3,5-di(*t*-butyl)-1,2,4-triphospholyl)$ZrCl_2$ (**6**) by chromatography on water deactivated silica led directly to **8** as the main organophosphorus product component, but in smaller isolable yield.

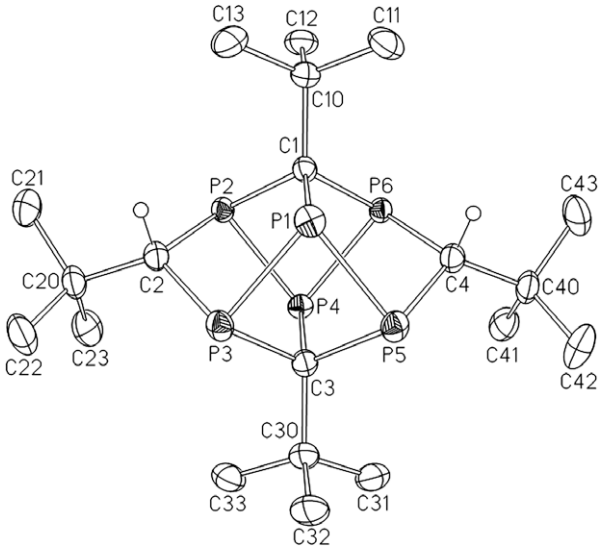

Fig. 9. Molecular structure of saturated $P_6(t\text{-BuC})_4H_2$ isomer **10**, in the solid state as determined as the majority component of a mixed crystal with its unsaturated isomer **10a** (ratio 0.954:0.046). *t*-Bu group hydrogen atoms are omitted for clarity. Selected bond distances [pm] and angles [°] for **10**: P(1)–P(3): 222.17(7); P(1)–P(5): 221.87(7); P(3)–C(2): 186.52(17); P(2)–C(2): 186.02(17); P(2)–C(1): 188.10(15); P(1)–C(1): 193.65(16); P(3)–C(3): 192.00(16); P(2)–P(4): 223.53(6); P(6)–C(1): 188.21(16); C(2)–P(3)–P(1): 92.54(6); P(3)–C(2)–P(2): 108.19(8); C(2)–P(2)–C(1): 99.90(7); C(1)–P(1)–P(3): 98.73(5); P(2)–C(1)–P(6): 93.99(7); P(5)–P(1)–P(3): 77.66(2); C(3)–P(3)–P(1): 86.02(5).

The reaction of Cp^*ZrCl_3 and 1-trimethylstannyl-3,5-di(*t*-butyl)-1,2,4-triphosphol (**3b**) [15] in toluene at room temperature led to the novel saturated cage **10**. It is another $P_6(t\text{-BuC})_4H_2$ isomer and can be related to Cp^*(η^5-3,5-di(*t*-butyl)-1,2,4-triphospholyl)$ZrCl_2$ as an observable intermediate. After stirring the reaction mixture overnight, the characteristic AB_2 spin system of an η^5-(3,5-di(*t*-butyl)-1,2,4-triphospholyl) complex (Table 1) appears as the prominent species in ^{31}P NMR spectroscopy besides other signals of organophosphorus compounds with dominating sp^3-hybridized P-nuclei. These NMR signals disappear slowly within two days and the typical signals of saturated P–C cage compounds become stronger. Column chromatography on water deactivated silica and *n*-hexane allowed the isolation of **10** as a red solid. Recrystallization from cold *n*-hexane resulted in reasonable 55% isolated yield of red prisms of the compound (Scheme 5).

^{31}P NMR spectroscopy immediately revealed a completely different bonding situation of **10** in relation to its isomers **8** and the saturated cage of Nixon [30] (Fig. 8). Both are chiral compounds. In contrast to that, **10** forms an $(AX_2)(BY_2)$ spin system for a saturated P–C cage compound with only weak $^{2}J_{PP}$ coupling between the two subsystems. The X_2 and Y_2 nuclei indicate magnetic equivalence for two pairs of P-nuclei. This is rather uncommon for a compound which is most probably formed by dimerization of the enantiomers of chiral **3c**. The ^{31}P NMR data are in good agreement with the molecular structure of **10** as determined in the crystalline state. Two chemically and magnetic inequivalent four-membered P_3C-rings indicated by hatched and bold bonds in the drawing of the molecule in Fig. 8 can be related to the AX_2 and BY_2 spin subsystems, but their correlation to each other is unclear in the moment. ^{1}H NMR of **10** fits to this model, ^{13}C is not very informative as the cage carbon atoms are missing due to strong P–C coupling.

X-ray diffraction studies on the red prisms of **10** revealed triclinic crystals in space group $P\bar{1}$. As the first investigated crystal

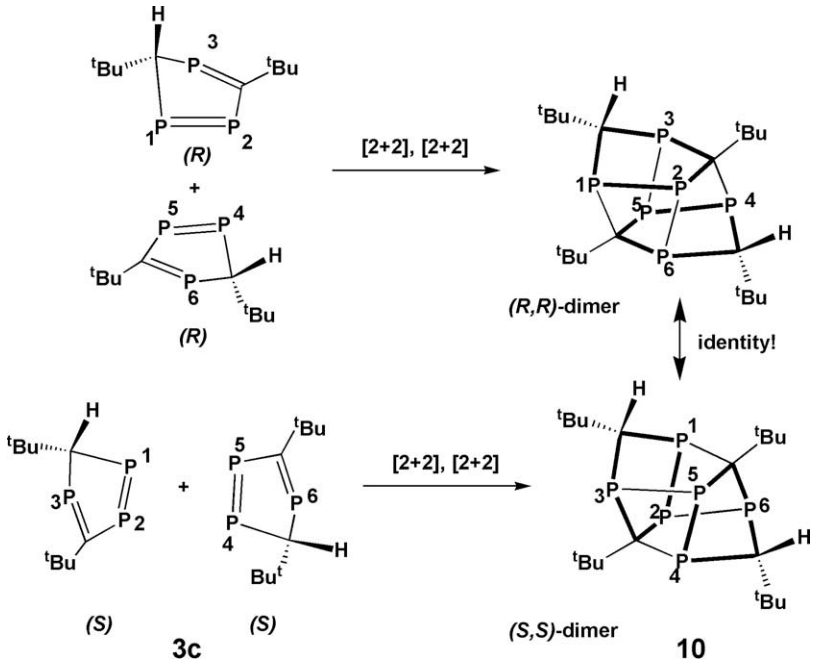

Scheme 6. Stereochemical considerations about the formation of *meso*-cage compound **10**.

contained 6.1% of another $C_{20}H_{38}P_6$ isomer **10a** in statistical distribution, the material was recrystallized again and reinvestigated but the content of the isomer was only marginally reduced to 4.6%. Isomer **10a** is chiral and contains one P=C double bond. Its molecular structure as deduced from differential data analysis is given in the Supplementary material. Due to its small contribution to the experimental data, the properties of **10a** shall not be discussed in this paper. The molecular structure of **10** is given in Fig. 9. The appearance of molecular cage compound **10** suggests a vertical mirror plane which is defined by the cage nuclei C(1), P(1), C(3), and P(4). All atomic parameters which are related in this way as for the pairs P(2)–P(6), P(3)–P(5), C(2)–C(4) and their respective bond lengths and angles are very close to σ_v-symmetry, but that is not realized in a crystallographic sense for the solid state. No chiral version of cage **10** is present in the crystal. The symmetry restrictions of the crystal disappear for solutions, thus

Table 2
Experimental data of X-ray diffraction studies.

	4	**5**	**6**	**8 + 9**	**10 + 10a**
Formula	$C_{15}H_{27}Cl_3P_2Zr$	$C_{20}H_{32}Cl_2P_2Zr$	$C_{15}H_{23}Cl_2P_3Zr$	$C_{20}H_{38.11}Cl_{0.12}P_6$	$C_{20}H_{38}P_6$
Crystal size (mm)	0.19 × 0.12 × 0.10	0.22 × 0.15 × 0.12	0.16 × 0.07 × 0.05	0.48 × 0.40 × 0.35	0.66 × 0.48 × 0.44
Crystal system	Monoclinic	Orthorhombic	Orthorhombic	Monoclinic	Triclinic
Space group	$P2_1/c$	$P2_12_12_1$	$P2_12_12_1$	$P2_1/n$	$P1$
a (pm)	966.7(1)	881.65(5)	673.37(3)	1085.0(1)	1022.4(1)
b (pm)	1499.7(1)	1557.24(9)	1503.4(2)	2039.7(3)	1091.5(1)
c (pm)	1445.8(2)	1608.54(9)	1930.0(2)	1238.8(1)	1245.3(1)
α (°)	90.0	90.0	90.0	90.0	106.960
β (°)	103.83(1)	90.0	90.0	106.58(1)	104.482
γ (°)	90.0	90.0	90.0	90.0	103.193
V (nm^3)	2.0351(2)	2.2084(2)	1.9538(3)	2.6276(5)	1.2171(2)
Z	4	4	4	4	2
M_r	466.88	496.52	458.36	468.52	464.32
μ (mm^{-1})	1.084	0.887	1.073	0.425	0.446
T_{min}/T_{max}	0.842/0.896	0.832/1.000	0.503/1.000	0.644/0.699	0.726/0.799
ρ (g cm^{-3})	1.524	1.4493	1.558	1.184	1.267
$F(000)$	952	1024	928	1000	496
T (data collected) (K)	100(2)	100(2)	100(2)	210(2)	200(2)
2θ Range (°)	$6.16 \leqslant 2\theta \leqslant 58.0$	$6.9 \leqslant 2\theta \leqslant 55.8$	$6.8 \leqslant 2\theta \leqslant 52.8$	$3.96 \leqslant 2\theta \leqslant 54.02$	$3.64 \leqslant 2\theta \leqslant 56.0$
hkl Range	$-13 \leqslant h \leqslant 13$	$-11 \leqslant h \leqslant 10$	$-8 \leqslant h \leqslant 7$	$-1 \leqslant h \leqslant 13$	$-1 \leqslant h \leqslant 13$
	$-20 \leqslant k \leqslant 20$	$-20 \leqslant k \leqslant 20$	$-18 \leqslant k \leqslant 18$	$-1 \leqslant k \leqslant 26$	$-13 \leqslant k \leqslant 13$
	$-19 \leqslant l \leqslant 19$	$-21 \leqslant l \leqslant 20$	$-23 \leqslant l \leqslant 24$	$-15 \leqslant l \leqslant 15$	$-16 \leqslant l \leqslant 16$
Reflections measured	34157	14234	16051	7013	6891
Reflections unique	5415	5058	3991	5727	5733
Reflections observed ($I \geqslant 2.0\sigma(I)$)	3689	3974	2967	3937	4460
Parameters refined	271	235	196	254	397
Goodness-of-fit (all data)	0.967	0.862	1.065	1.012	1.022
R_1 (observations reflected)	0.0438	0.0399	0.0542	0.0480	0.0301
wR_2 (all data)	0.0880	0.0814	0.1084	0.1196	0.0730
Absolute structure parameter [35]	–	0.03(5)	−0.08(9)	–	–

10 forms a true *meso*-compound there as indicated by NMR spectroscopy.

The uncommon effect of forming one single *meso*-dimer by cyclic addition of chiral triphosphole **3c** is related to the fact that the hydrogen atoms H(2) and H(4) share the same side of the cage with respect to the plane which is defined by the nuclei P(2), P(3), P(5), and P(6). The same accounts for the *t*-Bu groups of C(2) and C(4), which originally formed the stereogenic centers of triphosphole **3c**.

A stereochemical analysis of **10** with respect to **3c** revealed an interesting relationship between them. Compound **10** represents the dimerization product of two *R*-enantiomers or that of two of *S*-enantiomers of **3c** (Scheme 6)! Unlike the normal case of forming *meso*-compounds by combining the two optical antipodes of a chiral starting material, in this case it is the combination of two homochiral monomers which is identical for both enantiomeric versions of the monomer. The reaction sequences leading to **10** as well as to **8** and **9** share their remarkable preference for a highly selective dimerization of homochiral enantiomers of **3c**. It seems worthwhile to follow these stereochemical peculiarities of zirconium complex mediated cage forming processes in the future systematically for the stereoselective preparation of novel P–C cage compounds.

2.3. Catalytic oligomerization of 1-hexene with diphospholyl and triphospholyl zirconium π-complex catalysts

Catalytic oligomerization of 1-hexene was achieved with Cp(η^5-1,3-diphospholyl)$ZrCl_2$ complex (**5**) and Cp(η^5-1,2,4-triphospholyl)$ZrCl_2$ complex (**6**) with an excess of methylalumoxane (MAO) as the co-catalyst. The experimental setup follows a report of Janiak et al. who determined the relative reactivity of phosphole zirconium catalyst with respect to the basic catalytic system zirconocene dichloride [4]. A disadvantageous trend for the phospholyl derivatives of Cp_2ZrCl_2 is unluckily continued for its di- and triphospholyl analogues **5** and **6**: each additional phosphorus atom replacing a C–H unit of the catalyst diminishes the catalyst activity as well as the resulting turnover numbers. (TON: Cp_2ZrCl_2 = 16.666; **5** = 1.100; **6** = 68) The complete results are given in the Supporting information.

3. Conclusions

In this paper, we report for the first time about useful preparative routes to 1,3-diphospholyl and 1,2,4-triphospholyl zirconium π-complexes. Preparation and handling of the complexes requires consequent exclusion of moist and air. (η^5-2,4,5-Tri(*t*-butyl)-1,3-diphospholyl)$ZrCl_3$ (**4**), Cp(η^5-2,4,5-tri(*t*-butyl)-1,3-diphospholyl)-$ZrCl_2$ (**5**), and Cp(η^5-3,5-di(*t*-butyl)-1,2,4-triphospholyl)$ZrCl_2$ (**6**) are stable enough to be characterized fully under these circumstances. According to its NMR properties, **6** is one of the rare cases of a bent sandwich complex with non-rotating π-ligands outside the ansa-metallocenes, but **5** with its even more bulky 2,4,5-tri(*t*-butyl)-1,3-diphospholyl ligand shows no sign a hindered π-ligand rotation. This interpretation of the NMR experimental data seems to contradict the generally accepted rule for the conformational flexibility of π-complexes, where repulsive interactions between π-ligand substituents control the activation energy for ligand rotation. As an alternative model an attractive force between the π-ligands of **6** is discussed, which is generated by an interaction of two nucleophilic P-lone pairs with two electrophilic sp^2-ring carbon atoms of the Cp ligand.

Hydrolysis of (1,2,4-triphospholyl)Zr complexes or presence of moisture in the reaction mixture changes the course of the reactions completely and leads to oligo- or polycyclic organophosphorus compounds by dimerization of the hydrolysis product 3,5-di(*t*-butyl)-1,2,4-triphosphol **3c** to form $P_6(t\text{-BuC})_4H_2$ isomers as the main products. Depending on the starting materials and the reaction conditions either asymmetric tricyclic isomer **8** with two P=C double bonds is formed as a pair of enantiomers or *meso*-cage **10** as the only isolable stereoisomer. Surprisingly, both can be related to the dimerization of two homochiral molecules of (*R*)-3,5-di(*t*-butyl)-1,2,4-triphosphol **3c***R* or two units of its *S*-enantiomer. This means for the *meso*-compound **10**, an identical stereoisomer is formed by combining two *S*- or two *R*-enatiomers of **3c**, a very specific stereochemical situation. In both cases, no cyclic addition products have been identified, which would represent the heterochiral combination **3c***R* + **3c***S*.

P_2- and P_3-zirconocene dichloride derivatives **5** and **6** have been tested as Ziegler–Natta alkene oligomerization catalysts. Unluckily, the activity of the catalyst is reduced significantly by introducing isolobal P-atoms occupying the position of C–H fragments.

4. Experimental

4.1. General

All reactions were carried out in flame dried glassware, under an oxygen-free atmosphere of dry nitrogen using Schlenk techniques. Solvents were dried with the help of sodium or potassium ketyl radicals and distilled under N_2. All NMR solvents were carefully dried, degassed, and stored under N_2 over 4 Å molecular sieves. NMR spectra were recorded on JEOL JNM-EX 270, JNM-LA 400 and Bruker Avance DRX 300. ^1H and ^{13}C NMR chemical shifts are given relative to residual solvent peaks. ^{31}P NMR chemical shifts are referenced to external H_3PO_4 (85%). Mass spectra: Varian Mat 212 and JEOL JMS 700 spectrometers. Elemental analysis was performed locally by the microanalytical laboratory at the Department Chemie & Pharmazie of the University Erlangen-Nürnberg.

The starting materials were prepared as published: mixtures **2a**/**3a** [9], separation of $Na(THF)_n$ salts **2a** and **3a** with an average of n = 1.5 in both cases [10], and trimethylstannyltriphosphol **3b** [15]. Zirconium starting materials, NMR solvents, solvents for chemical reactions and chromatography, and static phases were purchased from standard commercial resources.

4.2. (η^5-2,4,5-tri(t-butyl)-1,3-diphospholyl)$ZrCl_3$ (4)

A suspension of 270 mg (0.75 mmol) sodium salt **2a** in 10 mL of toluene was syringed at room temperature to a stirred mixture of 175 mg (0.75 mmol) $ZrCl_4$ in 15 mL of toluene within 5 min. Throughout further stirring for an hour the color changed from brown to orange. Removal of the solvent in vacuum, addition of a few mL of *n*-hexane, filtration of the resulting solution and removal of the *n*-hexane in vacuum again led to the formation of the product as a yellow solid. Recrystallization from *n*-hexane resulted in the isolation of 160 mg (0.343 mmol, 46%) yellow **4**.

$^{31}P\{^1H\}$ NMR (121.5 MHz, toluene-d^8, RT): δ = 260.3 (s, 2P). ^1H NMR (300 MHz, toluene-d^8, RT): δ = 1.46 (s, 9H, $C(CH_3)_3$), 1.55 (s, 18H, $2C(CH_3)_3$). $^{13}C\{^1H\}$ NMR (75.5 MHz, toluene-d^8, RT): δ = 211.4 (t, $^1J(^{13}C, ^{31}P)$ = 72 Hz C(1)), 185.1 (X-part of an ABX spin system $\sum{}^1J(^{13}C, ^{31}P(A)) + {}^2J(^{13}C, ^{31}P(B))$ = 115 Hz C(2,3)), 41.8 (t, $^2J(^{13}C, ^{31}P)$ = 10.8 Hz C(5,6)), 41.5 (t, $^2J(^{13}C, ^{31}P)$ = 15.2 Hz C(4)), 35.3 (t, $^3J(^{13}C, ^{31}P)$ = 7.2 Hz C(7,8)), 34.7 (t, $^3J(^{13}C, ^{31}P)$ = 7.2 Hz C(9)). MS (FD, toluene): 270 [$P_3C_2{}^tBu_2$] (15%), 466 [M+] (7%), 541 [$H_2P_4C_6{}^tBu_6$] (100%). $C_{15}H_{27}Cl_3P_2Zr$ (466.79): Calc.: C, 38.59; H, 5.83. Found: C, 38.33; H, 6.85%.

4.3. Cp(η^5-2,4,5-tri(t-butyl)-1,3-diphospholyl)$ZrCl_2$ (5)

A suspension of 232 mg (0.632 mmol) sodium salt **2a** in 10 mL of toluene was syringed at room temperature dropwise to a stirred

mixture of 167 mg (0.97 mmol) $CpZrCl_3$ in 20 mL of toluene within 20 min. Throughout further stirring for an hour the color changed from brown-orange to yellow. Removal of the solvent in vacuum, addition of a few mL of *n*-hexane, filtration of the resulting solution and removal of the *n*-hexane in vacuum again led to the formation of the product as an orange solid. Dissolving the compound in refluxing *n*-hexane and recrystallization at room temperature resulted in the isolation of 180 mg (0.362 mmol 57%) orange **5**.

$^{31}P\{^1H\}$ NMR (121.5 MHz, toluene-d^8, RT): δ = 236.7 (s, 2P). ^1H NMR (300 MHz, toluene-d^8, RT): δ = 1.39 (s, 9H, $C(CH_3)_3$), 1.64 (s, 18H, $2C(CH_3)_3$), 6.35 (s, 5H, Cp). $^{13}C\{^1H\}$ NMR (75.5 MHz, toluene-d^8, RT): δ = 195.0 (t, $^1J(^{13}C, ^{31}P)$ = 69.8 Hz C(1)), 179.6 (X-part of an ABX spin system $\sum{}^1J(^{13}C, ^{31}P(A)) + {}^2J(^{13}C, ^{31}P(B))$ = 75.6 Hz C(2, 3)), 115.9 (s, C(Cp)), 39.9 (t, $^2J(^{13}C, ^{31}P)$ = 10.9 Hz C(5,6)), 39.4 (t, $^2J(^{13}C, ^{31}P)$ = 16.0 Hz C(4)), 34.2 (t, $^3J(^{13}C, ^{31}P)$ = 7.2 Hz C(7, 8)), 33.7 (t, $^3J(^{13}C, ^{31}P)$ = 7.8 Hz C(9)). MS (FD, toluene): 270 $[P_2C_3{}^tBu_3]$ (2%), 496 $[M^+]$ (50%), 541 $[H_2P_4C_6{}^tBu_6]$ (100%); $C_{20}H_{32}Cl_2P_2Zr$ (496.55): Calc.: C, 48.38; H, 6.50. Found: C, 47.84; H, 6.46%.

4.4. Cp(η^5-3,5-di(t-butyl)-1,2,4-triphospholyl)$ZrCl_2$ (6)

A suspension of 232 mg (0.636 mmol) sodium salt **3a** in 10 mL of toluene was syringed at room temperature dropwise to a stirred mixture of 347 mg (1.319 mmol) $CpZrCl_3$ in 20 mL of toluene within 20 min. Throughout further stirring for an hour the color changed from brown-orange to yellow. Removal of the solvent in vacuum, addition of a few mL of *n*-hexane, filtration of the resulting solution and slow and partial evaporation of the *n*-hexane in a stream of the inert gas led to the formation of small amounts of the target product as yellow needles. Attempt to workup the mother liquor which contained most of the yield failed due to the thermolability and hydrolytic instability of the compound, thus chemical yields of the reactions could not been determined.

$^{31}P\{^1H\}$ NMR (121.5 MHz, toluene-d^8, RT): δ = 282.5 (t, $^2J(^{31}P, ^{31}P)$ = 51.2 Hz 1P), 260.2 (d, $^2J(^{31}P, ^{31}P)$ = 51.2 Hz 2P). ^1H NMR (300 MHz, toluene-d^8, RT): δ = 1.56 (s, 18H, $C(CH_3)_3$), 6.12 (s, 3H, (C_5H_5)), 6.35 (s, 2H, (C_5H_5)). $^{13}C\{^1H\}$ NMR (75.5 MHz, toluene-d^8, RT): δ = 236.0 (dt, $^1J(^{13}C, ^{31}P)$ = 80 Hz, $\sum{}^1J(^{13}C, ^{31}P) + {}^2J(^{13}C, ^{31}P)$ = 98 Hz, C(1,2))), 119.3 (s, 3C, (C_5H_5)), 116.7 (t, $J(^{13}C, ^{31}P)$ = 2.2 Hz, 2C, (C_5H_5)), 44.4 (dt, $^2J(^{13}C, ^{31}P)$ = 18 Hz, $\sum{}^2J(^{13}C, ^{31}P) + {}^3J(^{13}C, ^{31}P)$ = 12 Hz, C(3,4)), 33.9 (dt, $^3J(^{13}C, ^{31}P)$ = 9 Hz, $\sum{}^3J(^{13}C, ^{31}P) + {}^4J(^{13}C, ^{31}P)$ = 8 Hz, C(5,6)). MS (FD, toluene): no signals associated with a Zr-complex of the heterocycle observable; $C_{15}H_{23}Cl_2P_3Zr$ (456.1): Calc.: C, 39.30; H, 5.06. Found: C, 39.80; H, 5.47%.

4.5. Unsaturated P_6(t-BuC)$_4H_2$ isomer exo-1,2,4,5,6,8-hexaphospha-3,7,9,10-tetra(tert-butyl)-tricyclo-[4.3.3.0]-3,9-decadien (8)

A suspension of 390 mg (1.068 mmol) sodium salt **3a** in 30 mL of toluene was syringed at room temperature dropwise to a stirred mixture of 272 mg (1.19 mmol) $ZrCl_4$ in 20 mL of toluene within 20 min. Refluxing of the reaction mixture for 6 h led to a color changed from yellow to orange and the formation of a colorless precipitate. ^{31}P NMR of the mixture proves the formation of a multiplicity of compounds with sp^2 and sp^3 hybridized phosphorus nuclei, but the absence of π-bound 1,2,4-triphospholyl ligands. The solvent was removed in vacuum and the remaining material dissolved in *n*-hexane. Column chromatographic workup on water deactivated silica (50 cm, 5% water) with *n*-hexane led to the formation of two yellow fractions. The first contains mainly the known saturated P_6(*t*-BuC)$_4H_2$ isomer [30] and the second one the two tricyclic organophosphorus compounds **8** and **9**. Removal of the solvent in vacuum and recrystallization from *n*-hexane (RT/−18 °C) led to the isolation of 85 mg (0.18 mmol, 33%) yellow mixed crystals consisting of 89% **8** and 11% **9**. Only repeated fractional recrystallization allowed the isolation of almost pure NMR samples of **8** in small amounts for an unambiguous determination of the spectroscopic parameters.

$^{31}P\{^1H\}$ NMR (121.5 MHz, toluene-d^8, RT): δ = 330 (d, $^2J(^{31}P, ^{31}P)$ = 31.5 Hz P(6)), 317 (pd, $^1J(^{31}P, ^{31}P)$ = 277 Hz P(1)), 31 (dd, $^1J(^{31}P, ^{31}P)$ = 277 Hz, $^1J(^{31}P, ^{31}P)$ = 309 Hz P(3)), 27 (pd, $^1J(^{31}P, ^{31}P)$ = 317 Hz P(2)), 18 (q, $^1J(^{31}P, ^{31}P)$ = 317 Hz, $^1J(^{31}P, ^{31}P)$ = 381 Hz P(5)), −18 (q, $^1J(^{31}P, ^{31}P)$ = 309 Hz, $^1J(^{31}P, ^{31}P)$ = 381 Hz P(4)). ^1H NMR (300 MHz, toluene-d^8, RT): δ = 1.07 (s, ^{t}Bu), 1.33 (s, ^{t}Bu), 1.41 (s, ^{t}Bu), 1.59 (s, ^{t}Bu). $^{13}C\{^1H\}$ NMR is hampered by the small amounts of available pure samples and strong P–C coupling for the ring C nuclei. MS (FD, toluene): *m*/*z* (%) = 500 (85) $[C_{20}H_{39}ClP_6]^+$, 464 (100) $[C_{20}H_{38}P_6]^+$. No correct analytical data could be obtained from the crystals.

4.6. Saturated P–C cage P_6(t-BuC)$_4H_2$ isomer (10)

A solution of 370 mg (0.937 mmol) trimethylstannyl-1,2,4-triphosphole derivative **3b** in 35 mL of toluene was syringed at room temperature dropwise to a stirred mixture 312 mg (0.937 mmol) Cp^*ZrCl_3 in 15 mL of toluene within 5 min. Stirring over night at RT led to a color changed from yellow to dark orange and the formation of a colorless precipitate. ^{31}P NMR of the mixture proves the presence of (η^5-1,2,4-triphospholyl)Zr complexes besides organophosphorus compounds with mainly sp^3 hybridized phosphorus nuclei. Stirring for additional two days at RT led to the disappearance of the π-complexes and an increase of intensity of the ^{31}P NMR signals of the organophosphorus components. Column chromatographic workup on water deactivated silica (50 cm, 5% water) with *n*-hexane yielded a yellow main fraction. Removal of the solvent and recrystallization from *n*-hexane (RT/−18 °C) led to the isolation of 120 mg (0.258 mmol, 55%) of red prisms of **10** which is polluted with ca. 5% of another P_6(*t*-BuC)$_4H_2$ isomer **10a**. Repeated recrystallization did not remove impurity **10a** significantly.

$^{31}P\{^1H\}$ NMR (121.5 MHz, toluene-d^8, RT): δ = −8.94 (t, $^1J(^{31}P, ^{31}P)$ = 123.9 Hz, 1P), 26.42 (t, $^1J(^{31}P, ^{31}P)$ = 139.6 Hz, 1P, 114.7 (d, $^1J(^{31}P, ^{31}P)$ = 123.9 Hz, 2P), 128.7 (d, $^1J(^{31}P, ^{31}P)$ = 139.6 Hz, 2P). ^1H NMR (300 MHz, toluene-d^8, RT): δ = 1.17 (s, 18 H, 2 ^{t}Bu), 1.23 (s, 18 H, 2 ^{t}Bu), 1.37 (s, 18H, ^{t}Bu), 2,89 (dd, $^2J(^1H, ^{31}P)$ = 6.6 Hz, $^2J(^1H, ^{31}P)$ = 10.4 Hz 2H, C–H_{cage}). $^{13}C\{^1H\}$ NMR is hampered by strong P–C coupling for the cage carbon nuclei. MS (FD, toluene): *m*/*z* (%): 464 (100) $[C_{20}H_{38}P_6]^+$. No correct analytical data could be obtained from the crystals.

4.7. Crystal structure determinations

Intensity data were collected on Bruker-Nonius KappaCCD (**4, 5, 6**) or Siemens P4 (**8, 9, 10**) diffractometers (φ- and ω-rotations) using Mo Kα radiation (graphite monochromator, λ = 0.71073 pm). Data were corrected for Lorentz and polarization effects. Absorption effects have been taken into account on a semi-empirical basis using multiple scans of equivalent reflections (SADABS, Bruker-AXS, 2002) [32,33]. All structures were solved by direct methods and refined by full-matrix least-squares procedures against F^2 with all reflections using SHELXTL-NT 5.10 (Bruker AXS, 1998) (**4, 8, 9, 10**) or SHELXTL-NT 6.12 (Bruker AXS, 2002) (**5, 6**) programs [34]. All non-hydrogen atoms were refined anisotropically. The positions of the hydrogen atoms were placed in positions of optimized geometry. The isotropic displacement parameters of all hydrogen atoms were tied to the equivalent isotropic displacement parameters of their corresponding carrier atoms by a factor of 1.2- or 1.5. Crystal data and experimental details are listed in Table 2.

Acknowledgements

This work was gratefully supported by grants of the Deutsche Forschungsgemeinschaft DFG.

Appendix A. Supplementary material

CCDC 699518, 699519, 699520, 699521, and 699521 contain the supplementary crystallographic data for **4**, **5**, **6**, **8** + **9**, and **10** + **10a,** respectively. These data can be obtained free of charge from The Cambridge Crystallographic Data Centre via www.ccdc.cam.ac.uk/data_request/cif. Supplementary data associated with this article can be found, in the online version, at doi:10.1016/j.jorganchem.2008.12.026.

References

[1] H.H. Brintzinger, D. Fischer, R. Mühlhaupt, B. Rieger, R.M. Waymouth, Angew. Chem., Int. Ed. Engl. 34 (1995) 1143;
W. Kaminsky, J. Chem. Soc., Dalton Trans. (1998) 1143.
[2] F.-X. Buzin, F. Nief, Francois, L. Ricard, F. Mathey, Organometallics 21 (2002) 259;
S. Bellemin-Laponnaz, M. Lo, M.-C. Michael, T.H. Peterson, J.M. Allen, G.C. Fu, Organometallics 20 (2001) 3453;
F. Nief, F. Mathey, L. Ricard, J. Organomet. Chem. 384 (1990) 271;
P. Meunier, B. Gautheron, J. Organomet. Chem. 193 (1980) C13–C16;
P. Desmurs, M. Visseaux, D. Baudry, A. Dormond, F. Nief, L. Ricard, Organometallics 15 (1996) 4178.
[3] E.J.M. de Boer, I.J. Gilmore, F.M. Korndorffer, A.D. Horton, A. Van der Linden, B.W. Royan, B.J. Ruisch, L. Schoon, R.W. Shaw, J. Mol. Catal. A: Chem. 128 (1998) 155;
T. Wada, Tooru, T. Tsukahara, T. Sugano, T. Takahama, H. Kurokawa, Jpn. Kokai Tokkyo Koho (1995). JP 07188335 A 19950725;
T. Tsukahara, T. Wada, T. Sugano, T. Takahama, K. Yamamoto, Jpn. Kokai Tokkyo Koho (1995). JP 07188319 A 19950725;
F.-X. Buzin, F. Nief, F. Mathey, Francois, J. Malinge, E. Deschamps, B. Deschamps, Int. Patent Appl. (2002). WO 2002059133 A1 20020801;
R.R. Ford, J.J. Vanderbilt, R.L. Whitfield, G.E. Moore, U.S. Pat. Appl. Publ. (2001). US 2001044505 A1 20011122;
K. Yokota, Kiyohiko. Eur. Pat. Appl. (1994). EP 590486 A2 19940406;
E.J.M. De Boer, H.J. Heeres, H.J.R. De Boer, Eur. Pat. Appl. (1995). EP 638593 A1 19950215;
T. Sugano, K. Yamamoto, Eur. Pat. Appl. (1996). EP 728773 A1 19960828;
J.A.M. Van Beek, G.H.J. Doremaele, K.A. Vandewiele, Y. Van Den Winkel, Yvar, Belg. Pat. Appl. (1995). BE 1007262 A3 19950502;
C. Janiak, U. Versteeg, K.C.H. Lange, R. Weimann, E. Hahn, J. Organometal. Chem. 501 (1995) 219;
M. Sone, A. Yano, Eur. Pat. Appl. (1993). EP 574794 A1 19931222;
L.V. Cribbs, J.A. Tyrell, S. Nagy, U.S. Pat. Appl. (2000). US 6121183 A 20000919.
[4] C. Janiak, K.C.H. Lange, P. Marquardt, J. Molecular Catal. A: Chemical 180 (2002) 43;
C. Janiak, K.C.H. Lange, P. Marquardt, R.-P. Kruger, R. Hanselmann, Macromol. Chem. Phys. 203 (2002) 129;
C. Janiak, K.C.H. Lange, U. Versteeg, D. Lentz, P.H.M. Budzelaar, Chem. Berichte 129 (1996) 1517.
[5] L.-S. Wang, T.K. Hollis, Org. Lett. 5 (2003) 2543.
[6] T. Aoki, S. Tadaya, Jpn. Kokai Tokkyo Koho (1995), JP 07070224 A 19950314; Eur. Pat. Appl (1994), EP 617052 A2 19940928.
[7] D. Hu, H. Schäufele, H. Pritzkow, U. Zenneck, Angew. Chem. 101 (1989) 929;
D. Hu, H. Schäufele, H. Pritzkow, U. Zenneck, Angew. Chem., Int. Ed. Engl. 28 (1989) 900;
M.M. Al-Ktaifani, W. Bauer, U. Bergsträßer, B. Breit, M.D. Francis, F.W. Heinemann, P.B. Hitchcock, A. Mack, J.F. Nixon, H. Pritzkow, M. Regitz, M. Zeller, U. Zenneck, Chem. Eur. J. 8 (2002) 2622.
[8] M. Hofmann, C. Höhn, F.W. Heinemann, U. Zenneck, Chem. Eur. J., submitted for publication.
[9] G. Becker, G. Gresser, W. Uhl, Z. Naturforsch. 36b (1981) 16.;
G. Becker, W. Becker, R. Knebl, H. Schmidt, U. Weeber, M. Westerhausen, Nova Acta Leopold. 59 (1985) 55.
[10] R. Bartsch, J.F. Nixon, Polyhedron 8 (1989) 2407.
[11] F.G.N. Cloke, J.R. Hanks, P.B. Hitchcock, J.F. Nixon, Chem. Commun. (1999) 1731.
[12] G.K.B. Clentsmith, F.G.N. Cloke, M.D. Francis, J.R. Hanks, P.B. Hitchcock, J.F. Nixon, J. Organomet. Chem. 693 (2008) 2287.
[13] P.B. Hitchcock, J.F. Nixon, R.M. Matos, J. Organomet. Chem. 490 (1995) 155.
[14] C.S.J. Callaghan, P.B. Hitchcock, J.F. Nixon, J. Organomet. Chem. 584 (1999) 87.
[15] A. Elvers, F.W. Heinemann, B. Wrackmeyer, U. Zenneck, Chem. Eur. J. 5 (1999) 3143.
[16] A. Bondi, J. Phys. Chem. 68 (1964) 441;
R.S. Rowland, R. Taylor, J. Phys. Chem. 100 (1996) 7384.
[17] L.F. Veiros, Organometallics 19 (2000) 5549.
[18] G. Erker, R. Nolte, G. Tainturier, A. Rheingold, Organometallics 8 (1989) 454.
[19] R. Bartsch, P.B. Hitchcock, J.F. Nixon, J. Chem. Soc., Chem. Commun. (1987) 1146;
R. Bartsch, F.G.N. Cloke, J.C. Green, R.M. Matos, J.F. Nixon, R.J. Suffolk, J.L. Suter, D.J. Wilson, J. Chem. Soc., Dalton Trans. (2001) 1013.
[20] M. Brym, M.D. Francis, G. Jin, C. Jones, D.P. David, A. Stasch, Organometallics 25 (2006) 4799.
[21] J. Okuda, E. Herdtweck, Chem. Ber. 121 (1988) 1899;
C.H. Winter, D.A. Dobbs, X.-X. Zhou, J. Organomet. Chem. 403 (1991) 145.
[22] R. Bartsch, P.B. Hitchcock, J.F. Nixon, J. Chem. Soc., Chem. Commun. (1990) 472.
[23] P.B. Hitchcock, R.M. Matos, J.F. Nixon, J. Organomet. Chem. 462 (1993) 319.
[24] L.H. Harrington, I. Vargas-Baca, N. Reginato, M.J. McGlinchey, Organometallics 22 (2003) 663;
Y. Ortin, K. Ahrensdorf, P. O'Donohue, D. Foede, H. Müller-Bunz, P. McArdle, A.R. Manning, M.J. McGlinchey, J. Organomet. Chem. 689 (2004) 1657.
[25] F.G.N. Cloke, K.R. Flower, P.B. Hitchcock, J.F. Niuxon, J. Chem. Soc., Chem. Commun. (1994) 489.
[26] C. Topf, T. Clark, F.W. Heinemann, M. Hennemann, S. Kummer, H. Pritzkow, U. Zenneck, Angew. Chem. 114 (2002) 4221;
C. Topf, T. Clark, F.W. Heinemann, M. Hennemann, S. Kummer, H. Pritzkow, U. Zenneck, Angew. Chem., Int. Ed. Engl. 41 (2002) 4047.
[27] L.M. Engelhardt, R.I. Papasergio, C.L. Raston, A.H. White, Organometallics 3 (1984) 18.
[28] A. Martin, M. Mena, F. Palacios, J. Organomet. Chem. 489 (1994) C10.
[29] K. Prout, T.S. Cameron, R.A. Forder, Acta Crystallogr. B 30 (1974) 2290.
[30] R. Bartsch, P.B. Hitchcock, J.F. Nixon, J. Chem. Soc., Chem. Commun. (1989) 1046.
[31] V. Caliman, P.B. Hitchcock, J.F. Nixon, J. Organomet. Chem. 536/537 (1997) 273.
[32] SADABS 2.08, Bruker AXS, Inc., Madison, WI, USA, 2002.
[33] P. Coppens, in: F.R. Ahmed, S.R. Hall, C.P. Huber (Eds.), Crystallographic Computing, Munksgaard, Copenhagen, 1970, p. 255.
[34] SHELXTL NT 6.12, Bruker AXS, Inc., Madison, WI, USA, 2002.
[35] H.D. Flack, Acta Crystallogr. A 39 (1983) 876.